

SLiMFast: Guaranteed Results for Data Fusion and Source Reliability

Manas Joglekar, Theodoros Rekatsinas, Hector Garcia-Molina, Aditya Parameswaran[†], Christopher Ré
Stanford University and [†] University of Illinois, Urbana-Champaign

ABSTRACT

We revisit data fusion, i.e., the problem of integrating noisy data from multiple sources by estimating the source accuracies, and show that the simple model of logistic regression can capture most existing approaches for solving data fusion. This allows us to put data fusion on a solid statistical footing and obtain solutions with rigorous theoretical guarantees. Expanding on logistic regression, we introduce SLiMFast, a framework that converts data fusion to a learning and inference problem over discriminative probabilistic models. In contrast to previous approaches that rely on complex generative models, discriminative models allow us to decouple the specification of a data fusion model from the algorithm used to learn the model’s parameters. This allows us to extend data fusion to take into account domain-specific features that are indicative of the accuracy of data sources, and design data fusion approaches that yield source accuracy estimates with $5\times$ lower error than competing baselines. We also design an optimizer to automatically select the best algorithm for learning the model’s parameters. We validate our optimizer on multiple real datasets and show that it chooses the best algorithm for learning in almost all cases.

1. INTRODUCTION

Integrating information from multiple data sources is crucial for maximizing the value extracted from data. Different data sources can provide information about the same *object*, e.g., a real-world entity or event, but information from different sources about the same object may be in conflict. Thus, *data fusion*—the task of resolving conflicts across sources by estimating their reliability—has emerged as a key element of data integration [10]. Interacting with our collaborators at Stanford Hospital—who are currently engaged in extracting information from the literature to populate a structured data repository—we find that applying data fusion in practice still poses a challenge for non-expert users despite the numerous approaches proposed in the literature [4, 6, 12, 18, 19, 26, 37]. We use the application of our collaborators as an example to demonstrate the challenges users face due to limitations of current data fusion approaches and motivate our approach.

Example 1. A genomics expert from Stanford Hospital wants to extract gene mutations associated to genetic diseases from a corpus of 22 million PubMed articles. The expert’s goal is to use this data to diagnose patients with Mendelian disorders. To this end, the expert extracts (gene, disease, associated) tuples from the articles where the field “associated” takes values in {true, false}. An article can be viewed as providing a set of triples that make claims about gene-disease associations. In many cases, the extracted triples may contain conflicts. For instance, the sentences

“Variation in *GIGYF2* is not associated with Parkinson disease”¹ and “These data strongly support *GIGYF2* as a *PARK11* gene with a causal role in familial Parkinson Disease”² will yield conflicting extractions. The expert wants to use data fusion to resolve such conflicts and obtain only gene-disease associations most likely to be correct according to the literature.

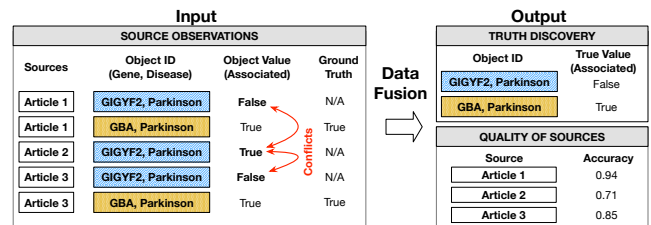


Figure 1: A schematic diagram of data fusion when extracting gene-disease associations from scientific articles.

For exposition purposes, we view articles as data sources. Other notions of sources, such as a research lab or a journal, can be naturally captured in the framework described below. Triples (gene, disease, associated) can be viewed as objects with the *gene-disease* pair being the object’s id and *associated* the object’s value. Consequently, the extracted (gene, disease, associated) tuples from each article correspond to observations from this source (i.e., the article) for the objects. Data fusion resolves conflicts by estimating the reliability of data sources and using that to infer the true value of each object. The reliability of a data source is captured using the notion of *source accuracy*, i.e., the probability that the source provides correct information. Figure 1 shows an overview of the input and output of data fusion. The input is a set of source observations and the output consists of the estimated source accuracies and the true values of objects. In certain cases, limited ground truth on the correctness of source observations may be available and can be used to obtain an initial estimate on the accuracy of data sources. **The Need for Guarantees.** Continuing with our example, the domain expert wants to use the extracted data for patient diagnosis. Due to the critical nature of the diagnosis application, formal guarantees on the correctness of the objects in the final knowledge base are required. As a result, data fusion should also provide formal guarantees that the returned gene-disease associations are correct within a certain margin of error.

One approach to obtain guarantees is having access to a sizable amount of labeled (or ground truth) data used to estimate source accuracies. However, obtaining large volumes of labeled data can

¹<http://www.neurology.org/content/72/22/1886.abstract>

²<http://www.ncbi.nlm.nih.gov/pubmed/18358451>

be prohibitively expensive due to the monetary cost associated with human annotators. Hence, most existing data fusion approaches assume no ground truth data. This forces them to rely on procedures such as *expectation maximization* (EM) to estimate the accuracy of data sources. These procedures come with few theoretical guarantees on their convergence and may yield suboptimal solutions [36]. The above raises the key technical question we seek to address, i.e., *how much ground truth is actually needed to obtain high-quality results with formal guarantees?* We show that under certain conditions, which match our target applications, only a surprisingly small amount of ground truth data is sufficient to obtain data fusion techniques that simultaneously (i) identify the correct values of objects with high-confidence, and (ii) obtain low-error (in many cases less than 2%) estimates of source accuracies. Low-error accuracy estimates have their merits in intelligence applications [29, 30] and can also help users minimize the monetary cost of data acquisition by purchasing only accurate data sources [8].

The Need for Domain Knowledge. *The expert believes that findings in some articles may not be trustworthy altogether and wants to use additional external knowledge about the sources themselves to estimate their accuracy better and further improve the quality of data fusion. Information such as the citation count or publication year can be informative of the accuracy of article claims. More fine-grained information such as the experimental design of a study can also be informative. For instance, the genomics expert definitely trusts results of gene-knockout studies, but is skeptical about genome-wide association studies (GWAS).*

We later demonstrate how domain knowledge can be integrated in data fusion in the form of *domain-specific features* that are indicative of a data source having high or low accuracy. Current data fusion methods do not take into account such features but only use the conflicting observations across sources to estimate their accuracy. Moreover, existing methods rely on complex models that are not easily extensible to incorporate domain-specific features.

The Need for Scalability. *To obtain a high-quality database the expert has to refine the design of the information extraction pipeline iteratively. The faster each iteration the higher the quality of the final output will be. Thus, if data fusion is to be incorporated in extraction pipelines considering many data sources, it needs to scale to large number of data sources and objects.*

As discussed earlier most data fusion methods use unsupervised procedures such as EM. These are expensive procedures that do not scale to large inputs. Furthermore, the run-time complexity of some more sophisticated methods (e.g., methods that capture source dependencies) is quadratic in the number of data sources [6]. As we discuss later the presence of ground truth allows us to use highly-efficient techniques leading to data fusion methods with significantly better scalability properties.

Apart from the expert in Genomics, we also interviewed experts in Applied Micro-Economic Theory, and a consumer electronics company, all engaged in extracting facts from the scientific literature to support analytic applications. All requirements outlined above were unanimously identified as important across all domains. These requirements were also outlined in a recent survey by Li et al. [21] as open problems for data fusion. We show how a simple data fusion approach can address most of these open problems.

Our Approach. To address these challenges, we introduce SLiM-Fast, a framework that relies on discriminative probabilistic graphical models to perform data fusion. At its simplest form, SLiM-Fast’s model corresponds to *logistic regression*. This formulation separates data fusion into two tasks: (i) performing *statistical learning*

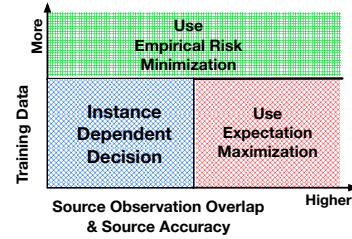


Figure 2: The tradeoff space SLiM-Fast’s optimizer captures to select the best algorithm for learning the source accuracies.

to compute the parameters of the graphical model—used to estimate the accuracy of data sources—and (ii) performing *probabilistic inference* to predict the true values of objects. Using graphical models for data fusion is not new [4, 6, 12, 26, 37]. However, SLiM-Fast comes with several advancements over previous work:

(1) SLiM-Fast is the first data fusion approach to combine cross-source conflicts with domain-specific features—integrated as additional variables in SLiM-Fast’s graphical model—to solve data fusion more effectively. We show that, for multiple real-world applications, combining these two types of signals can yield F1-score improvements of more than 50% when predicting the true value of objects and can lead to $5\times$ lower error in source accuracy estimates.

(2) We show that most of the existing data fusion models can be captured by the discriminative model of logistic regression, and thus, can be subsumed by SLiM-Fast. Moreover, we show that when SLiM-Fast’s underlying graphical model corresponds to logistic regression, SLiM-Fast can provably identify the correct value of objects and obtain low-error estimates of the true source accuracies when limited ground truth data is available; in our experimental evaluation we show that in certain cases as few as 10 training examples are sufficient to obtain F1-score higher than 0.8. Our theoretical analysis builds upon existing learning theory results [25].

(3) To learn the parameters of SLiM-Fast’s graphical model, one can either use expectation maximization (EM) or leverage the presence of ground truth and use empirical risk minimization (ERM). The performance of the two algorithm depends on specific characteristics of the input data. Our theoretical analysis indicates that ERM’s performance depends on the amount of *ground truth data*, while EM can estimate the source accuracies correctly when there is significant *overlap across source observations* and when the *average accuracy of sources* is high. This introduces a tradeoff between EM and ERM in terms of which algorithm can estimate the source accuracies better. To obviate the need for non-expert users to choose between EM and ERM, we design a lightweight optimizer that analyzes this tradeoff and selects which algorithm will obtain the best estimates for source accuracies. An overview of the tradeoff and the corresponding optimizer decisions is shown in Figure 2.

To choose between EM and ERM, our optimizer analyzes the information available to each algorithm for estimating the source accuracies. While ERM leverages the information in *ground truth data*, EM uses the information captured in *source conflicts*. Assuming that one ground truth data point contains one unit of information, we design a statistical model that analyzes the data fusion input to estimate the equivalent *units of information in source conflicts*. This gives us a mechanism to compare EM and ERM.

We evaluate our optimizer on multiple real-world datasets with varying properties, and show that in almost all cases it selects the best performing algorithm correctly. Due to this optimizer, SLiM-Fast does not require users to have any machine learning proficiency. They only need to provide the necessary input to SLiM-Fast and do not need to focus on the algorithm used to solve data fusion.

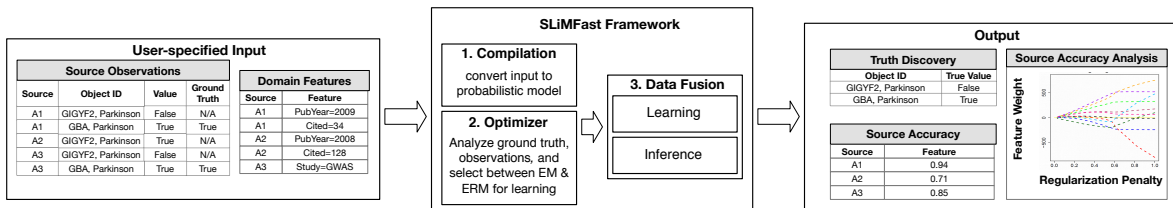


Figure 3: An overview of SLiMFAST’s core components. The provided source observations and domain-specific features are compiled into a probabilistic model used to solve data fusion via statistical learning and probabilistic inference.

$$w(s) : \text{Observations}(s,o,v_{o,s}) \wedge T_o = v_{o,s}$$

$$w(k) : \text{Observations}(s,o,v_{o,s}) \wedge \text{DomainFeatures}(s,k) \wedge T_o = v_{o,s}$$

Figure 4: SLiMFAST’s compilation as factor graph templates over the input source-observations and source features tables.

Summary of Contributions. We propose SLiMFAST, a framework that converts data fusion to a learning and inference problem over a simple discriminative probabilistic model. We show how SLiMFAST addresses several of open-problems in data fusion outlined by Li et al. [21]. In Section 2, we describe SLiMFAST and show how it subsumes existing data fusion methods, thus, obviating the need of *model selection*. In Section 3, we obtain strong guarantees on the performance of SLiMFAST, thus, establishing a series of *theoretical guarantees* for data fusion. Our analysis indicates that one can obtain high-quality solutions with limited ground truth, which, in turn, allows us to solve data fusion *efficiently*. We also design an optimizer that given a set of source observations as input, automatically selects the best algorithm for learning the parameters of SLiMFAST’s graphical model (Section 4). We evaluate the effectiveness of SLiMFAST and its optimizer on multiple real datasets (Section 5). Finally, we explore some extensions of SLiMFAST and discuss how it can be used to solve the problem of *source reliability initialization* and how it can be integrated in pipelines that extract information from unstructured text (Section 6).

2. THE SLiMFAST FRAMEWORK

We first review the problem of data fusion and then introduce SLiMFAST. At the end of the section, we discuss SLiMFAST’s connection to existing data fusion models.

2.1 Data Fusion Setup

We consider the same setup as in Example 1. We have a set of objects denoted by O . Each object $o \in O$ is associated with an attribute whose value v_o^* is unknown. We denote the domain of v_o^* as D_o . For instance, the gene-disease pair (GIGYF2, Parkinson) from Example 1 corresponds to an object whose attribute *associated* has an unknown value in $\{\text{true}, \text{false}\}$. For exposition purposes, we assume that for all objects $D_o = \{\text{True}, \text{False}\}$; this can be easily extended to other settings.

We also have a set of data sources denoted by S (e.g., articles in Example 1). Each source provides observations, i.e., assigns values to a subset of objects. For example, in Figure 1, source “Article 2” asserts that “GIGYF2” is “truly” associated with “Parkinson”. Formally, an observation from source $s \in S$ for an object $o \in O$, denoted by $v_{o,s}$, is a mapping from the source-object pair (o, s) to a value in D_o . We use Ω to denote the set of all source observations. A source can provide wrong observations for objects, thus, different source observations can assign conflicting values to the same object (see Figure 1). An observation $v_{o,s}$ is wrong if $v_{o,s} \neq v_o^*$. To measure the correctness of the observations provided by a source we use the notion of accuracy. The true accuracy of a source s ,

denoted by A_s^* , is the probability that the information provided by s is correct [6, 37]. Accuracies are also unknown.

Finally, we may have ground truth information for some source observations, i.e., we know if $v_{o,s} \neq v_o^*$ or $v_{o,s} = v_o^*$. For instance, in Example 1, we know that the assertion from Article 1 that “GBA” is “truly” associated with “Parkinson” is correct. Given O, Ω and S , the goal of data fusion is to estimate the unknown accuracies of data sources and determine the true values of objects. In Example 1, data fusion estimates the accuracy of “Article 1” to be 0.94 and determines that “GIGYF2” is not associated with “Parkinson”.

2.2 Overview of SLiMFAST

An overview of SLiMFAST is shown in Figure 3. The input to SLiMFAST consists of two tables: (i) a table with source-object observations and potential ground truth (if available) on their correctness, and (ii) a user-specified table containing domain-specific features that are indicative of the accuracy of data sources. Revisiting Example 1, these features can correspond to the experimental methodology used for the study described in an article, the number of citations, publication year of an article, and so on. An example of a set of input features is shown in table “Domain Features” in Figure 3. For simplicity, we assume that domain-specific features are binary. Categorical features can be converted to binary by introducing a separate feature for each value, while real-valued features can be converted to categorical and then binary using bucketization.

The given input is compiled to a probabilistic graphical model. Then SLiMFAST’s optimizer analyzes the input to determine the best algorithm for learning the parameters of the logistic regression model. Finally, learning and inference are performed over the graphical model to solve data fusion.

Compilation. SLiMFAST compiles the two input tables into a probabilistic graphical model. For each object $o \in O$ we have a random variable T_o taking values in D_o that is associated with the unknown true value v_o^* of the object. Apart from the domain-specific features, SLiMFAST also introduces an *indicator feature* for each data source s taking the value 1 for source s and 0 for other sources. We denote the set of domain-specific features and indicator features as K . For each source $s \in S$ and feature in $k \in K$ we have an observed variable $f_{s,k} \in \{0, 1\}$ denoting the value of feature k for source s . Let F denote the source-feature matrix containing all variables $f_{s,k}$.

Let Ω_o be the set of all observations for an object, i.e., all (o, s) pairs for which $v_{o,s} \in \Omega$. To determine the true value of an object we compute the posterior probability $P(T_o = d | \Omega_o, F)$ for all values $d \in D_o$, and assign T_o the one with the highest probability. SLiMFAST follows a *discriminative* approach that models the posterior $P(T_o | \Omega_o, F)$ directly. In the remainder of the paper, we focus on the cases where SLiMFAST uses a softmax model to estimate the posterior probability

$$P(T_o | \Omega_o, F; w) = \exp\left(\sum_{s \in \Omega_o} \sum_{k \in K} w_k f_{s,k} v_{o,s}\right) / Z \quad (1)$$

where Z is a normalization constant, and $w = \langle w_k \rangle_{k \in K}$ are the model parameters capturing the importance of source features. This naturally generalizes the case of source independent accuracies due to the indicator features. SLiMFAST assumes that model parameters are coupled across features. When variables T_o are binary then Equation 1 corresponds to a *simple logistic regression model*.

SLiMFAST uses a *factor graph* representation to capture the above probabilistic model. Factor graphs can model a wide range of probability distributions using two types of nodes: (i) *variables*, which can be either evidence variables when their value is known, or query variables when their value should be predicted, and (ii) *factors*, which are local functions that define the relationships between variables in the graph. Figure 4 shows a rule-based, first-order logic representation of the factor templates used by SLiMFAST to compile the input source-observation and source-feature tables to the underlying factor graph. The first rule associates each source observation variable $v_{o,s}$ with the appropriate variable T_o and effectively captures source indicator features. The second rule extends the model with domain-specific features $f_{s,k}$. Rule weights correspond to the parameters w in Equation 1. Any declarative factor graph framework (e.g., Alchemy [1], DeepDive [2], PSL [16]) can be used to express SLiMFAST’s underlying probabilistic model.

Solving Data Fusion with SLiMFAST. To solve data fusion one needs to (i) learn the parameters w by optimizing the likelihood $\ell(w) = \log P(T|\Omega, F; w)$ where T corresponds to a set of variables T_o , and (ii) infer the maximum a posteriori (MAP) assignments to variables T_o . For learning, we can either use expectation maximization (EM) [32, 34] or empirical risk minimization (ERM) [24] when ground truth is available. For EM, the likelihood ℓ is taken over all unobserved variables $T_o, \forall o \in O$, and thus, corresponds to a non-convex objective. EM jointly learns the parameters w and the distribution of T_o that maximize the likelihood ℓ in an iterative fashion, hence, leading to an expensive algorithm. On the other hand, in the presence of ground truth, the likelihood ℓ is taken over the observed variables T_o in the ground truth. This yields a convex objective for ERM, thus, highly-efficient methods such as stochastic gradient descent (SGD) can be used to learn w . SLiMFAST’s optimizer (Section 4) analyzes the input ground truth and source observations to determine which of EM or ERM will yield better estimates of the data source accuracies, and thus, allow SLiMFAST to determine the true values of objects more accurately.

After learning, the data source accuracies are estimated as $A_s = 1/(1 + \exp(-\sum_{k \in K} w_k f_{s,k}))$ where A_s denotes the estimated accuracy of source s . This connection will become apparent in Section 2.3. Finally, we perform probabilistic inference to obtain the marginal probability of variables T_o and sample those to obtain the true values for objects. Apart from the traditional output for data fusion, SLiMFAST also analyzes the impact of domain-specific features on the quality of sources (see Section 5.5). Learning and inference can be performed within the framework used to express SLiMFAST’s probabilistic model. We used the DeepDive framework [2, 33]. In DeepDive, both EM and ERM are implemented over the highly-scalable stochastic gradient descent procedure. Probabilistic inference is performed via Gibbs sampling. DeepDive’s highly-efficient sampler [38] allows us to obtain efficient data fusion models that seamlessly scale to large instances.

2.3 SLiMFAST and Existing Fusion Methods

Many existing approaches convert data fusion to a learning and inference problem over probabilistic graphical models [4, 6, 12, 26, 37]. The main difference between SLiMFAST and previous meth-

ods is that *SLiMFAST relies on a discriminative probabilistic model while previous methods rely on generative probabilistic models*. This means that in contrast to SLiMFAST which estimates the posterior probability of variables T_o directly, previous approaches learn the joint distribution $P(T_o, \Omega_o)$ following a Naive Bayes model.

We focus on the most common data fusion approach first and discuss more sophisticated approaches later. Previous methods do not consider domain-specific features, thus, we only consider source observations. We associate a random variable $V_{o,s}$ with each source observation $v_{o,s}$. Applying Bayes rule, the posterior $P(T_o|\Omega_o)$ is $P(T_o|\Omega_o) = P(T_o)P(\Omega_o|T_o)/Z$ where Z is a normalizing constant. Under the assumption that data sources are independent we have $P(\Omega_o|T_o) = \prod_{(o,s) \in \Omega_o} P(V_{o,s}|T_o)$. From the definition of source accuracy $P(V_{o,s}|T_o)$ is given by

$$P(V_{o,s}|T_o) = \begin{cases} A_s^* & \text{if } T_o = V_{o,s} \\ 1 - A_s^* & \text{if } T_o \neq V_{o,s} \end{cases}$$

To solve data fusion, one can use EM to find the assignments of A_s and T_o that maximize the joint likelihood

$$\prod_{o \in O} P(T_o) \prod_{(o,s) \in \Omega_o} P(V_{o,s}|T_o; A_s)$$

The discriminative equivalent of Naive Bayes is *logistic regression* [25]. In fact, when $V_{o,s}$ are boolean, Naive Bayes and logistic regression are exactly the same [24]. Logistic regression describes the conditional distribution of a binary dependent variable Y via a logistic function over a vector of predictor variables (features) \mathbf{X} . We have $P(Y = 1|X) = \sigma(w_0 + \mathbf{w} \cdot \mathbf{X})$ where $\sigma(z) = 1/(1 + e^{-z})$ is the logistic function and w_0, \mathbf{w} the weights (i.e., parameters) of the model. Let $P(Y = 1) = \pi, P(X_i|Y = 1) = \theta_{+i}$, and $P(X_i|Y = 0) = \theta_{-i}$. The logistic regression and Naive Bayes are the same if weights w_0 and w_i are set to

$$w_0 = \sigma \left(\log \left(\frac{\pi}{1 - \pi} \right) + \sum_i \log \left(\frac{1 - \theta_{+i}}{1 - \theta_{-i}} \right) \right)$$

$$w_i = \log \left(\frac{\theta_{+i}(1 - \theta_{-i})}{\theta_{-i}(1 - \theta_{+i})} \right)$$

The Naive Bayes formulation of data fusion shown above is subsumed by logistic regression when $Y = T_o, \mathbf{X} = \langle V_{o,s} \rangle_{(o,s) \in \Omega_o}, P(T_o) = \pi, \theta_{+(o,s)} = A_s^*, \theta_{-(o,s)} = 1 - A_s^*$, and all weights $w_{(o,s)}$ are coupled to the same value $w_{(o,s)} = w_s = 2 \log \left(\frac{A_s^*}{1 - A_s^*} \right)$. From the above we have that $A_s^* = 1/(1 + \exp(-w_s/2))$. Similarly, when sources are associated with domain-specific features their accuracy is given by $\sigma(-\sum_{k \in K} w_k f_{s,k})$.

Logistic regression subsumes more sophisticated data fusion models. For instance, the Bayesian data fusion model by Zhao et al. [40] that differentiates between type-I and type-II errors made by sources can be subsumed by logistic regression since parameters θ_{+s} and θ_{-s} can naturally capture the true positive and false positive rate of a data source. In Section 6, we demonstrate how logistic regression can capture some data fusion models that consider copying between data sources [6].

Discussion. Since SLiMFAST relies on the general framework of factor graphs, it can subsume many of the existing data fusion models. Data fusion can be naturally viewed as a *classification problem*. Thus, one can follow the *discriminative relaxation* procedure introduced by Patel et al. [28] to convert potentially more complicated generative data fusion models to their discriminative counterparts which, in turn, can be represented as a factor graph. While simple, this realization, combined with SLiMFAST’s optimizer, obviates

the need for non-expert users to select an appropriate data fusion model for different data fusion tasks, thus addressing the problem of model selection from Li et al. [21].

While generative models usually come with strong distributional assumptions (e.g., Naive Bayes for data fusion assumes that source observations are conditionally independent), discriminative models relax some of the distributional assumptions to the reduce bias. For example, if conditional independence is violated, logistic regression will adjust the weights to account for cross-source correlations [25]. If sufficient training data is available then a discriminative model will achieve better performance on a specific task. Moreover, as we discuss in the next section, discriminative models allow us to obtain rigorous guarantees on recovering their true parameters via learning and to bound the error of their predictions.

3. THEORETICAL ANALYSIS

We build upon existing learning theory results to obtain guarantees on data fusion solutions. We provide guarantees on SLiM-Fast’s output in the presence of ground truth and also extend our discussion to cases where no ground truth is available. The results in this section are used by our optimizer (Section 4) to select the best algorithm during learning. A background discussion on existing results we build upon and the proofs for all theorems below can be found in the Appendix of the paper.

3.1 Guarantees on SLiM-Fast’s Output

We state guarantees on SLiM-Fast’s ability to obtain low-error estimates for the accuracy of data sources and its ability to predict the true value of each object correctly.

Guarantees on Source Accuracies. We start with formalizing the way we measure SLiM-Fast’s performance for estimating the true accuracy of sources. SLiM-Fast’s model is parameterized by a weight vector w of length $|K|$ containing the values w_k for each feature $k \in K$. We assume that source-object pairs (s, o) (and a corresponding true object value v_o^* and observation $v_{s,o}$) are drawn from some unknown probability distribution \mathcal{D} . Let \mathcal{D}_S denote the probability distribution over sources obtained from \mathcal{D} . Let $L(w)$ denote the loss of a model with weight vector w which quantifies how bad its source accuracy estimates are with respect to distribution \mathcal{D} . We use log-loss for this purpose.

Definition 2 (Accuracy Estimate Loss). *The loss of a weight vector w , denoted L_w , is defined as:*

$$L_w = E_{(s,o) \sim \mathcal{D}}[L_w(s, o)]$$

where

$$L_w(s, o) = I_{V_{o,s}=v_o^*} \log(A_s(w)) + I_{V_{o,s} \neq v_o^*} \log(1 - A_s(w))$$

I is the indicator function, and as discussed in Section 2

$$A_s(w) = 1 / (1 + \exp(-\sum_{k \in K} w_k f_{s,k}))$$

Loss L_w can also be written as:

$$L_w = E_{s \sim \mathcal{D}_S} [A_s^* \log(A_s(w)) + (1 - A_s^*) \log(1 - A_s(w))]$$

where A_s^* denotes the true unknown accuracy of a data source. This quantity is minimized when $A_s(w) = A_s^*$ for each s , and the difference from its optimal value is the expected Kullback-Leibler (KL) divergence between the true accuracy A_s^* and the predicted accuracy $A_s(w)$. We now state our bound on the accuracy estimation error.

Theorem 1. *Let G be a set of n training examples sampled from distribution \mathcal{D} . Let*

$$w^* = \operatorname{argmin}_w L_w \text{ and } w = \operatorname{argmin}_w \sum_{(s,o) \in G} L_w(s, o)$$

Then with high probability,

$$L_w \leq L_{w^*} + O(\sqrt{|K|/n} \log(n)) \quad (2)$$

This theorem follows from known results on Rademacher complexity (detailed in Appendix A). While similar in form to generalization results for classification the loss L here is parameterized by w . Our optimizer uses the error estimate provided by this theorem for determining when to use ERM. To gauge the impact of this theorem on our accuracy estimation error, we consider two cases:

Perfect Features: Consider the case when the true source accuracies are exactly equal to a logistic function of the features, i.e., for all $s \in S$, we have $A_s^* = 1 / (1 + \exp(\sum_{k \in K} w_k^* f_{s,k}))$. Then $L_w - L_{w^*}$ is simply $E_{s \sim \mathcal{D}_S} \text{KL}(A_s(w) || A_s^*)$, i.e., the expected value of the KL divergence between the true and predicted accuracies. This divergence is bounded by $O(\sqrt{|K|/n} \log(n))$, so it decreases approximately as the square root of the number of training examples.

Using the fact that $\text{KL}(A_1 || A_2) \geq (A_1 - A_2)^2 / 2$, we can bound the L_2 error of our accuracy estimates

$$E_{s \sim \mathcal{D}_S} [(A_s^* - A_s(w))^2] \leq O(\sqrt{|K|/n} \log(n))$$

Model Mismatch: In this case the true source accuracies are not exactly generated by a logistic function with w^* . So, the KL divergence with the true accuracies does not go to 0 even in the limit of infinite training examples. Let the *model mismatch coefficient* be given by $C_M = E_{s \sim \mathcal{D}_S} \text{KL}(A_s(w^*) || A_s^*)$. This measures the expected KL divergence between the best prediction achievable by the model (w^*) and the true accuracies. Then our bound tells us that $E_{s \sim \mathcal{D}_S} \text{KL}(A_s(w) || A_s^*) \leq C_M + O(\sqrt{|K|/n})$. As long as the predictions of w^* are not too far from the true accuracies, i.e., as long as C_M is small, the excess risk will still decrease as the square root of n , and saturate at C_M for large n .

Our bound states that the KL divergence is proportional to $\sqrt{|K|}$. This suggests that adding extra, potentially uninformative features to our model can significantly worsen our source accuracy estimates. In Appendix C, we show a result that lets us perform feature selection via sparsity inducing regularization methods [3] and maintain a low-error rate.

Guarantees On the True Value of Objects. Given an weight assignment w for SLiM-Fast’s probabilistic model and a set of source-observations Ω , we can compute the posterior probability of each variable T_o being true, denoted by $P_w(T_o | \Omega, F)$, by performing probabilistic inference. Then our loss function when inferring the true values of objects is:

Definition 3 (Object True Value Loss). *The object true value loss L_O of a weight vector w is defined as:*

$$L(w) = \frac{1}{|O|} \sum_{o \in O} I_{v_o^*=1} \log(P_w(T_o | \Omega, F)) + I_{v_o^*=0} \log(1 - P_w(T_o | \Omega, F))$$

For a random training set G_O of l objects the log-loss is:

$$L_G(w) = \frac{1}{l} \sum_{o \in G_O} I_{v_o^*=1} \log(P_w(T_o | \Omega, F)) + I_{v_o^*=0} \log(1 - P_w(T_o | \Omega, F))$$

We have the following result:

Theorem 2. *With high probability over the random choice of G_O :*

$$L(w) \leq L_G(w) + O(\sqrt{|K|/l} \log(l))$$

The theorem states that the log-loss over all objects is not much larger than the log-loss over the training set G_O . Building upon this result, we have that if we learn the model weights w by optimizing over the log-loss $L_G(w)$ and if $\sqrt{|K|/l}$ is small, we will infer the correct true values of all objects with high-probability.

3.2 Analyzing Source Conflicts

We now analyze data fusion when relying solely on the conflicts across source observations for estimating the source accuracies. While we are able to obtain theoretical guarantees only for a restricted scenario, our analysis forms part of the basis on which we build SLiMFAST’s optimizer in the next section.

We consider a set of data sources S providing observations on a set of objects O . Let A_s^* denote the true accuracy of source $s \in S$. Additionally, we make the following assumptions:

- The accuracy of each source s takes values in $[0.5 + \delta/2, 1 - \delta/2]$ for some $0 < \delta \leq 0.5$.
- Sources have *uniform selectivities*. That is, for each source-object pair (s, o) , there is a probability p that source s provides an observation for object o . We also assume that $p \geq 2/|S|$, i.e., in expectation, at least two sources talk about any object. The expected number of source-object observations is $|S||O| \cdot p$.
- We consider a set of K features that are predictive of the accuracies of data sources.

Theorem 3. *If all above conditions hold we can obtain an estimate A_s for the accuracy of source s such that $\frac{1}{|S|} \sum_{s \in S} KL(A_s || A_s^*) \leq O(\log(|O|)/(|S|\delta) + \sqrt{k/|O||S|p} \log^2(|O||S|/\delta))$ where KL stands for the KL divergence.*

The error depends on two properties of a fusion instance: (i) the true accuracy of sources, and (ii) the overlap across source observations. The higher the source accuracies are (i.e., the higher the value of δ) the lower the estimation error will be. The same holds for the source overlap (controlled via p). In the next section, we quantify the source overlap via the notion of *density*, defined as the *average fraction of data sources providing observations for an object*. We also extend the above to a general model for estimating if EM can learn the parameters of SLiMFAST’s model accurately.

4. THE SLiMFAST OPTIMIZER

We study the tradeoff space that SLiMFAST’s optimizer considers to select between EM and ERM during learning. We introduce an information theoretic model for comparing the performance of EM and ERM and describe the core-algorithm of SLiMFAST’s optimizer.

4.1 Overview

Given a collection of source observations, and some ground truth data, the goal of SLiMFAST’s optimizer is to select between EM and ERM for learning. Since ERM is always faster than EM, our optimizer compares the performance of EM and ERM on obtaining low-error estimates for the true source accuracies and retrieving the correct value of objects correctly.

ERM performs better as more ground truth data becomes available. On the other hand, our analysis indicates that EM can estimate the source accuracies accurately when the average true accuracy across data sources is high and there is sufficient overlap across source observations. We use (i) the amount of training data available, (ii) the average accuracy of data sources, and (iii) the density

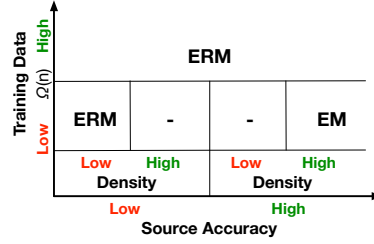


Figure 6: The tradeoff space for SLiMFAST’s optimizer. Dash indicates that the best algorithm varies.

of the fusion instance, i.e., the average fraction of data sources providing observations for an object, to describe the tradeoff space for SLiMFAST’s optimizer. We use synthetic data to demonstrate the effect of each dimension on EM and ERM.

Example 4. *Consider a data fusion instance with 1,000 sources and 1,000 objects. Sources are assumed to be independent. We evaluate the performance of EM and ERM on retrieving the true value of each object. We vary the average source accuracy in $[0.5, 0.8]$, the amount of training data in $[\text{.1\%}, 60\%]$, and density in $[0.005, 0.02]$. ERM is always faster than EM with runtimes ~ 30 sec and ~ 115 sec respectively. However, the best-performing algorithm differs as the three parameters change.*

We start by comparing the performance of EM and ERM as we vary the amount of training data while keeping other dimensions fixed. The results are shown in Figure 5(a). As expected for very small amounts of ground truth data EM outperforms ERM, but as the ground truth data increases ERM performs better.

We now focus on a regime with limited training data as one would expect in real applications. Figures 5(b) and 5(c) show the effect of varying the density and accuracy of data sources on the performance of EM and ERM while keeping other instance parameters fixed. When the ground truth on source-observations and the average accuracy are fixed, EM outperforms ERM for more dense instances. EM also outperforms ERM as the average source accuracy increases but the density and amount of training data remain fixed. Figure 6 shows the tradeoff space that SLiMFAST’s optimizer considers. For certain regions of the space, determining the best performing algorithm is not trivial, thus, we develop a model that collectively analyzes all three factors discussed above to determine which of the two learning algorithms will perform better.

4.2 Learning Method Selection

ERM relies exclusively on the presence of ground truth to learn the model parameters. The theoretical analysis in Section 3 establishes the amount of labeled examples as a proxy for determining if ERM will learn a model that can correctly predict the true values of objects and obtain low-error estimates of source accuracies. Our bounds consider ground truth on source-object observations being correct or false. This inherently captures the density of the data fusion instance. For example, if we know the true value of an object with 10 sources providing observations for this object we have 10 training examples. EM relies on the information captured in conflicting data source observations. To understand the properties of EM better, we consider the steps followed by the algorithm: EM alternates between: (i) the expectation step (E-step) where objects are probabilistically assigned a true value according to their posteriors (conditioned on source accuracies and observations), and (ii) the maximization step (M-step) where the model parameters are assigned their maximum likelihood values. Comparing EM to ERM,

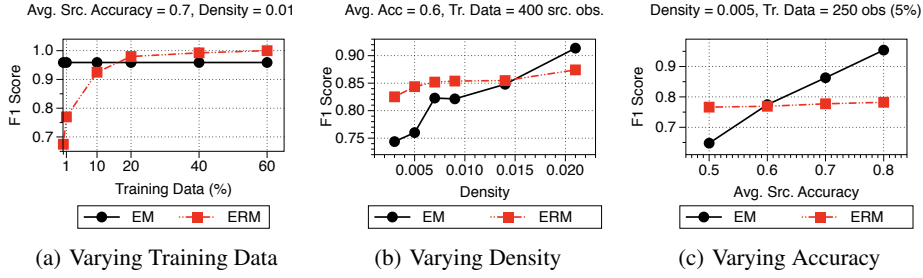


Figure 5: EM versus ERM as we vary (a) the amount of ground truth, (b) the density, and (c) the average accuracy of data sources. ERM is less sensitive to the fusion instance characteristics. EM performs better for more accurate sources and more sense instances.

we see that they only differ on the presence of the E-step. ERM also performs an M-step where the model parameters are assigned their maximum likelihood values with respect to ground truth. This leads to the key observation that *if we can compare the information in the output of the E-step with the information in the ground truth we can compare the performance between EM and ERM.*

Comparing EM with ERM. First we consider the information obtained from ground truth data. Given an object o and the random variable T_o from our data fusion model, we define a Boolean random variable C_o taking the value true if variable T_o obtains the correct value for o and the value false otherwise. If we have no access to ground truth data the maximum value of C_o 's entropy is $H(C_o) = 1$. Given ground truth information on T_o the entropy of C_o becomes $H(C_o) = 0$, thus, we gain 1-unit of information. If we have m sources providing observations for object o , the total information gain is m -units for this object. Summing these quantities over all objects in the ground truth data, we obtain the total units of information gain. We now apply a similar procedure to estimate the information we gain after the E-step of EM. We use a simple example to illustrate the high-level intuition:

Example 5. Consider an object o whose true value is unknown, and $m = 10$ data sources providing observations for it. Assume all sources have the same accuracy $p = 0.7$ and a simple majority vote model for resolving conflicts across sources. Majority vote retrieves the correct value for o if more than $m/2$ sources provide the correct value. The probability p_e of this event occurring is given as a function of the CDF of a Binomial distribution parameterized by p , m and $m/2$:

$$p_e = 1 - \sum_{i=0}^{m/2} \binom{m}{i} p^i (1-p)^{m-i} = 0.8497 \quad (3)$$

We now consider the random variable C_o from above. Given p_e the probability that variable C_o becomes true is p_e and we have $H(C_o) = -p_e \log_2(p_e) - (1-p_e) \log_2(1-p_e) = 0.611$. Thus, after applying the majority vote model during the E-step, object o contributes 0.389-units of information. Multiplying that with m we have that object o contributes a total of 3.89-units.

Generalizing Example 5, we model the E-step of EM via a majority vote model making the simplifying assumption that all data sources have the same accuracy. The probability that this model will obtain the correct value for an object is measured via the CDF of a Binomial distribution. Finally, to estimate the total number of information units we iterate over all objects. Algorithm 1 shows an overview of the procedure.

Estimating the Average Source Accuracy. Algorithm 1 assumes the average accuracy of data sources as input. However,

Algorithm 1: EMUnits: Estimating Information Units for EM

Input: Objects O , Source Observations Ω , Average Source Accuracy p

Output: EM Information Units

$totalUnits = 0$;

for each object in O do

$m =$ total #sources with observations for o ;

$$p_e = 1 - \sum_{i=0}^{m/2} \binom{m}{i} p^i (1-p)^{m-i};$$

if $p_e \geq 0.5$ then

$totalUnits +=$

$$1 - p_e \log_2(p_e) - (1-p_e) \log_2(1-p_e);$$

return $totalUnits$;

this information is not directly available. We describe an algorithm based on matrix completion for estimating this quantity. Given the set of source observations Ω , we define X to be an $|S| \times |S|$ matrix capturing the *agreement rate* of data sources. Given a data source s let O_s denote the set of objects for which s provides an observation. We define entry $X_{i,j}$ for sources s_i and s_j as

$$X_{i,j} = \frac{1}{|O_{s_i} \cap O_{s_j}|} \sum_{o \in O_{s_i} \cap O_{s_j}} I[v_{o,s_i} = v_{o,s_j}] - I[v_{o,s_i} \neq v_{o,s_j}]$$

For simplicity we assume that all data sources have the same accuracy p and that they are not adversarial, i.e., $p > 0.5$. Given p the expected agreement rate between s_i and s_j is given by $p^2 + (1-p)^2 - 2p(1-p) = (2p-1)^2$. Let $\mu = 2p-1$. It is easy to see that $E[X_{i,j}] = \mu^2$. Therefore we can estimate μ as $\hat{\mu} = \arg \min \frac{1}{2} \|X - \mu^2\|_2$ which corresponds to a matrix completion problem. Setting the derivative of the optimization objective to zero gives as the closed form solution $\hat{\mu} = \sqrt{\frac{\sum_{i,j} X_{i,j}}{|S|^2 - |S|}}$. Given $\hat{\mu}$ we get $p = (\hat{\mu} + 1)/2$. One can extend this setup to learn a different accuracy per source. Stochastic gradient descent (SGD) can be used to solve the corresponding matrix completion problem efficiently. In fact, recent work by De Sa et al. has shown that SGD is guaranteed to converge globally, thus, allowing us to estimate the source accuracies correctly [31].

Overall Algorithm. The core algorithm in SLiMFast's optimizer is shown in Algorithm 2. As shown, it considers the estimated EM units and the amount of ground truth labels to choose between EM and ERM. Following our theoretical analysis, we first examine if the bound in Equation 2 is below a threshold τ . If so, then we always choose to use the ERM algorithm. Otherwise we compare the amount of ground truth data with the estimated EM

units (Algorithm 1) to decide between EM and ERM. In Section 5 we evaluate our optimizer on different real world datasets and show that it selects the best algorithm almost every time. Our optimizer runs in 2% (\sim 3secs) of the total time required to solve data fusion.

Algorithm 2: SLiMFast’s Optimizer

Input: Objects O , Source Observations Ω , Source Features K , Ground Truth G , Threshold τ
Output: Learning Algorithm
if $\sqrt{|K|/|G|} \log(|G|) < \tau$ **then**
 \perp return ERM;
 $totalERMUnits = |G|$;
Estimate Average Source Accuracy p ;
 $totalEMUnits = EMUnits(O, \Omega, p)$;
if $totalERMUnits < totalEMUnits$ **then**
 \perp return EM;
else
 \perp return ERM;

Discussion. When a large amount of labeled data is available one can estimate the accuracy of sources with low-error as the empirical fraction of erroneous observations per source. The standard error guarantees apply. Nonetheless, we still use ERM for SLiM-Fast, as learning the source accuracies in isolation corresponds to a Naive Bayes model and the conditional independence assumption for sources may not apply in practice (see Section 5).

5. EXPERIMENTAL EVALUATION

We evaluate the performance of SLiMFast and our optimizer on multiple scenarios. The main points we seek to validate are: (i) how much training data is needed to obtain high-quality data fusion models, (ii) what is the impact of domain-specific features on data fusion, and (iii) how effective is SLiMFast’s optimizer in selecting between EM and ERM for learning the parameters of SLiMFast’s probabilistic model. Finally, we investigate how SLiMFast’s output can be used to provide insights on source accuracies.

5.1 Experimental Setting

We describe the datasets and experimental setting used below.

Datasets. We validate the performance of SLiMFast on three datasets, one from the finance domain, one from the intelligence domain, and a crowdsourcing dataset. In the first two, the sources are web-domains and for the third the sources are crowd-workers.

Stocks. In this dataset sources provide information on the volume of stocks, i.e., the total number of shares that trade hands from sellers to buyers, for a day in July 2011. It was obtained by a dataset generated by Li et al. [20] containing stock data for every day during July 2011. We picked a random day and focused on stock volumes as they exhibit the most conflicts across sources. We removed sources that are no longer active and for which no traffic statistics could be obtained (see discussion on domain-specific features below), and removed highly-accurate sources (e.g., NASDAQ) used to obtain ground truth data.

Demonstrations. This dataset contains reports of demonstrations in Africa from January, 2015 to April, 2015 from GDELT [17], a catalogue with daily extractions of real-world events from online news articles. Sources correspond to online news domains. The same demonstration can be reported by multiple sources. However, the corresponding GDELT entries can contain conflicts (e.g.,

Table 1: Parameters of the data used for evaluation.

Parameter	Stocks	Demonstrations	Crowd
# Sources	34	522	102
# Objects	907	3105	992
# Observations	30763	27736	19840
# Domain-Specific Features	7	7	4
# Distinct Feature Values	70	341	171
Avg. Source Accuracy	< 0.5	0.604	0.54
Avg. Observations per Object	33.9	15.703	20
Avg. Observations per Source	904.79	53.13	194.51

report different dates or lat-long coordinates) due to extraction errors. We associate each extraction with an object taking values in {True, False} and our goal is to determine the correct extractions. Ground truth was obtained using the ACLED dataset³. ACLED is a human curated database of demonstrations in Africa. To generate ground truth data, we mapped each GDELT entry to an ACLED entry, such that the date and location of the two entries are the same. The ACLED data is assumed to be complete, i.e., any demonstration not in ACLED is assumed to be false.

Crowd. For our last dataset we used the “weather sentiment” dataset from Crowdflower⁴. The dataset contains crowd evaluations for the sentiment of weather-related tweets corresponding to *positive*, *negative*, *neutral*, and *not weather related*. The dataset contains 1000 tweets and contributions from 20 different workers per tweet. Our goal is to detect the true sentiment for each tweet. Ground truth evaluations are provided together with the raw data.

Table 1 shows statistics characterizing the above datasets. For all datasets we follow the single truth semantics, i.e., an object can only take one true value from its domain.

Domain-specific Features. For the first two datasets, sources correspond to web-domains. We associate each domain to seven traffic statistics obtained by Alexa.com: (i) global rank, (ii) country rank, (iii), bounce rate, (iv) daily page views per visitor, (v) daily time on site, (vi) search visits, and (vii) total sites linking in. All metrics take numeric values and are discretized to generate Boolean features. We found that discretization does not affect SLiMFast’s performance significantly. For the third dataset, the features are (i) the channel of each worker, i.e., the particular market used to hire the worker, (ii) the country and (iii) city of the worker, and (iv) the fraction of tweets labeled by the worker.

Implementation Details. All models were implemented in the DeepDive framework [33]. We used Greenplum to handle the data loading and manipulation. The statistical inference and learning code were all written in C++. All experiments were executed on a machine with four CPUs (each CPU is a 12-core 2.40 GHz Xeon E5-4657L), 1TB RAM, running Ubuntu 12.04.

Methods. We compare the performance of three versions of SLiM-Fast against different baselines.

- **SLiMFast-ERM, SLiMFast-EM, SLiMFast-OPT:** The first two always use ERM and EM respectively to learn the parameters of SLiMFast’s model. The last uses SLiMFast’s optimizer to select between EM and ERM.
- **Counts:** This method corresponds to a Naive Bayes data fusion approach. Ground truth is used to learn the accuracy of each source in isolation by computing the fraction of times the source provides the correct value for objects with ground truth information. This method is highly-efficient as only count operations are performed during learning but is expected to yield high-errors when sources are not independent

³<http://www.acleddata.com>

⁴<http://www.crowdflower.com/data-for-everyone>

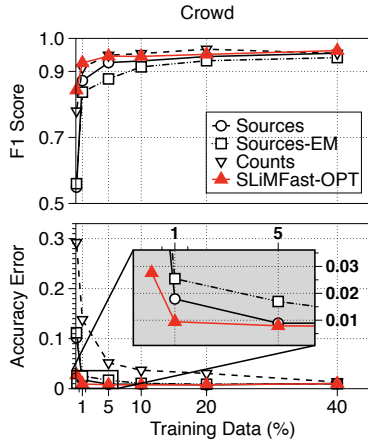


Figure 7: Comparing the performance of SLiMFAST-OPT against Sources, SourcesEM, and Counts for Crowd.

and only a very small amount of training data is available.

- **Sources:** The same as SLiMFAST but without domain-specific features. ERM is always used to learn the model-parameters.
- **Sources-EM:** The same as Sources but EM is used to learn the model-parameters. This approach corresponds to existing data fusion models used in prior work [6, 7, 21].

EM is implemented on top of DeepDive’s sampler using stochastic gradient descent to optimize the likelihood objective. Any available ground truth is used to initialize the model parameters.

Evaluation Methodology. We evaluate each method for different training-testing splits by revealing part of the labelled examples to the model. The percentage of training data takes values in $\{0.1\%, 1\%, 5\%, 10\%, 20\%, 40\%\}$. The splits are generated randomly, thus, for each training-testing split we execute each method five times and report its average performance. To measure performance we use the following metrics:

- **F1-score:** used to measure how well each method infers the true value of objects. We evaluate the performance of methods only for objects in the testing data.
- **Error on Estimated Accuracies:** a weighted-average of the absolute estimation error across all source accuracies. For each source we take the absolute error between its estimated accuracy and its true accuracy. The true accuracies are computed using the entire ground truth data. Errors are weighted by the number of observations per source.
- **Runtime:** the wall-clock runtime measured in seconds.

5.2 The Effect of Domain-Specific Features

We start by evaluating the effect of domain-specific features on the output of data fusion. We validate our theoretical result that domain-specific features can yield high-quality solutions to data fusion with only small amounts of ground truth. Intuitively, the presence of domain-specific features enables SLiMFAST to capture correlations across data sources that share the same features. We expect SLiMFAST to yield higher-quality solutions than baselines that do not take domain-specific features into account, especially for small amounts of ground truth.

Figure 7 shows the F1-score and estimation error for source accuracies obtained by all methods for Crowd. When the amount of training data is small, i.e., less than 5%, domain-specific features lead to significant improvements both for the F1-score and the estimation error. The effect of domain-specific features is evident

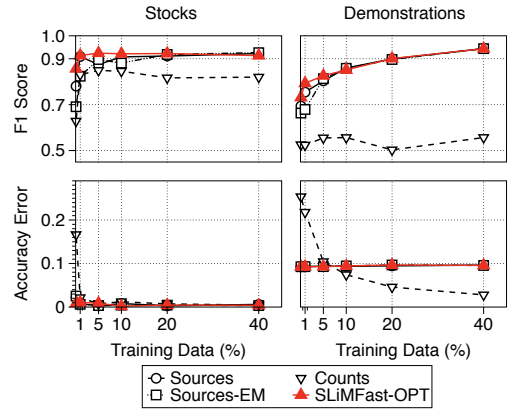


Figure 8: Comparing SLiMFAST-OPT against Sources, SourcesEM, and Counts for Stock and Demonstrations.

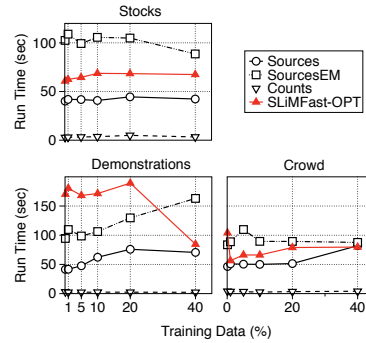


Figure 9: Comparing the runtime of SLiMFAST-OPT against Sources, SourcesEM, and Counts.

if we compare the scores obtained by Sources and Sources-EM to the score of SLiMFAST-OPT with 0.1% training data. We see that SLiMFAST-OPT yields an improvement of around 50%. Providing slightly more ground truth, i.e., 1% (around 10 objects), SLiMFAST-OPT yields an F1-score of more than 0.9. SLiMFAST-OPT also exhibits lower estimation-error for source accuracies. For small amounts of training data, SLiMFAST-OPT obtains 2× to 5× lower error estimates for source accuracies. For higher amounts of ground truth all algorithms perform similarly.

We observe similar results for Stock and Demonstrations; shown in Figure 8. When the ground truth is limited, SLiMFAST-OPT yields a smaller but still significant F1-improvement (10%) compared to the best performing baseline. One interesting point is that for Demonstrations, Counts obtains better estimates for the accuracy of sources when more than 10% of the training data is used. However, the F1-score obtained by Counts is significantly smaller than the score for other methods. We attribute this to the fact that the conditional independence assumption made by Counts—recall that it corresponds to Naive Bayes—does not hold for Demonstrations (see Section 6).

Take-away. Domain-specific features allow us to retrieve good solutions with a notably small amount of training data. Obtaining small amounts of ground truth is feasible for most real-world applications. In these cases, SLiMFAST can identify the true value of objects more accurately than existing data fusion models and can also obtain lower error estimates for the accuracy of sources.

5.3 Overall Runtime

We report the total wall-clock runtime of each algorithm for all datasets in Figure 9. Reported runtimes for Sources, SourcesEM in-

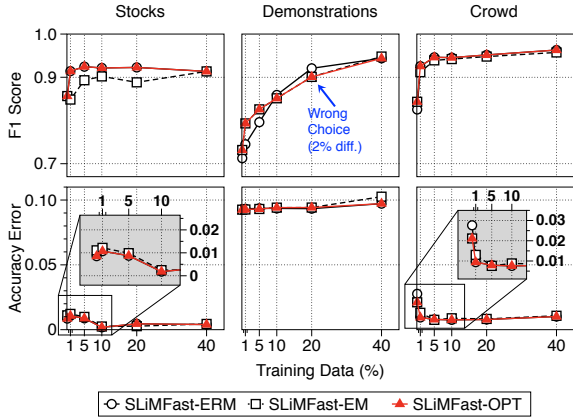


Figure 10: Validating SLiMFAST’s optimizer. In almost all cases the optimizer selects the best algorithm for learning.

clude the time required to compile the input data to the corresponding data fusion model. As expected non-EM based approaches are much faster. We see that leveraging the presence of ground truth information allows us to obtain more scalable data fusion models that perform as good or better than EM based approaches. We would like to remind the reader that our EM implementation is already optimized for speed as it is implemented on top of DeepDive’s sampler and leverages gradient descent.

5.4 Evaluating SLiMFAST’s Optimizer

We evaluate the performance of SLiMFAST’s optimizer. Figure 10 reports the F1-score, and accuracy estimation error of SLiMFAST, SLiMFAST-EM, and SLiMFAST-OPT. We set the threshold parameter τ in Algorithm 2 to 0.1.

For Stocks the density, i.e., the probability of a source providing an observation for an object, is 0.99. The average accuracy of data sources is below 0.5. As expected from our analysis in Section 4, ERM indeed obtains a better F1-score than EM for all amounts of ground truth data. Our optimizer correctly selects to execute the ERM algorithm during learning for all amounts of ground truth.

For Crowd the density drops to 0.196. However, the average accuracy increases to 0.54. EM obtains a better F1-score and lower estimation error only for very small amounts of ground truth data, i.e., 0.1%. Once more data is available, ERM outperforms EM on both metrics. We see that our optimizer is capable of picking up this change and correctly switches to the better ERM algorithm.

For Demonstrations is a sparse dataset with density 0.06 and an average source accuracy of 0.6. EM outperforms ERM when fewer than 10% of the ground truth is revealed. As shown our optimizer correctly selects EM for all these cases. When more than 10% of ground truth is revealed, ERM is a better choice than EM as it obtains a better F1-score and is also faster. For 10% training data EM and ERM are comparable but for 20% ERM outperforms EM. Our optimizer makes a mistake and chooses EM for both cases.

Finally, we vary the threshold parameter $\tau \in \{1.0, 0.5, 0.1, 0.01\}$ to evaluate the robustness of our optimizer. For Stock, our optimizer correctly selects to always run ERM for all values of τ . Similarly for Crowd it makes no mistakes as it correctly switches to ERM after 1% of training data is revealed for all values of τ . For Demonstrations and $\tau \geq 0.5$ our optimizer selects to run EM for $\leq 5\%$ of ground truth and ERM afterwards, thus, making no mistake. For $\tau = \{0.01\}$, our optimizer switches to EM only for 40% of training data, hence, making two mistakes.

Take-away. SLiMFAST’s optimizer can effectively choose between the best algorithm for learning in almost all cases. Our experi-

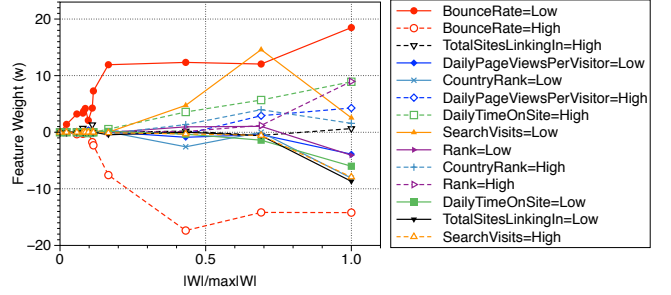


Figure 11: Lasso path for features used in Stocks. Higher x -axis values correspond to lower regularization penalties.

mental evaluation reveals that the simple model described in Section 4.2 can accurately detect which of the learning algorithms, EM or ERM, will perform better for a variety of data fusion instances.

5.5 Obtaining Insights on Data Source Quality

Controlling the regularization penalty when learning the weights of domain-specific features allows non-expert users to understand which of them are informative. One of the most prominent methods for performing this task in probabilistic models is to compute the *regularization path* [11, 35] for the model in hand. That is, compute the coefficient of each feature used in the model while ranging the magnitude of the regularization penalty from larger to smaller values. Such plots enable non-expert users to understand the impact of each feature on the accuracy of sources.

SLiMFAST uses l_1 -regularization, i.e., it penalizes the overall objective by a term $\lambda|W|$. When λ is zero, there is no penalization, and all features tend to have non-zero weights, thus, the quantity $|W|/\max|W|$ takes larger values. Moreover, the most important features should have significantly higher weights. As the penalization λ increases, $|W|$ is pulled towards zero (and so $|W|/\max|W|$), with the less important parameters being pulled to zero earlier. At some level of λ , all feature weights will be pulled to zero. The x -axis on the regularization path graph corresponds to $|W|/\max|W|$ while the y -axis the weight of each feature. Using these plots, important features are expected to have non-zero weights for larger penalties and their weights are expected to increase as the penalty decreases. This allows users to identify the most informative features in their application.

The regularization path for Stocks is shown in Figure 11. Higher values on the x -axis correspond to lower regularization penalties. The order at which features obtain non-zero weights, i.e., their *activation order*, and their coefficient are indicative of how informative each feature is. Interestingly, the most informative features correspond to daily usage statistics, such as the “Bounce Rate” (with low bounce rate implying higher accuracy), the “Daily Page Views” (with low views implying low accuracy), etc. It is interesting to observe that the number of “Total Sites Linking In”, i.e., a proxy for PageRank, is activated early but does not have a high-value coefficient. This is in accordance with a recent result by Dong et al. [7] that shows how the accuracy of websites is not correlated with PageRank. The lasso path for Crowd is shown in Appendix D.

6. EXTENSIONS

We briefly describe certain extensions of SLiMFAST to more sophisticated tasks related to data fusion.

Copying Sources. We validate that more sophisticated models considering data copying across sources can be implemented in SLiMFAST. We chose the source-copying approach by Dong et

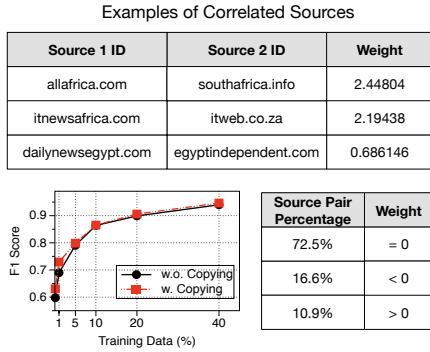


Figure 12: Detecting correlated sources for Demonstrations.

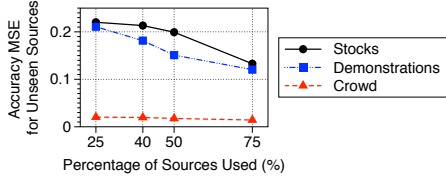


Figure 13: Using features to estimate source accuracy.

al. [6]. The intuition for copying is that if two sources make the same mistakes then the probability of copying is high.

We extended SLiMFAST’s compilation module to capture the aforementioned intuition with the following factor template: $w_c(s, s') : \text{Observations}(s, o, v_{o,s}) \wedge \text{Observations}(s', o, v_{o,s'}) \wedge v_{o,s} = v_{o,s'} \neq T_o$. It is easy to see that since T_o is the only unknown variable the underlying factor graph remains a logistic regression model with an additional feature considering pairs of data sources.

We focused on Demonstrations where sources correspond to online news portals. We compare the F1-score obtained by the copying model with the regular data fusion model that considers only data sources. No domain-specific features were used. The results are shown in Figure 12. Adding copying leads to better performance. Some statistics on the amount of correlations across sources are shown in Figure 12. Our copying data fusion model discovers that there are indications of copying in around 10% of all source pairs. Examples are shown in the table in the same figure. Domains from the same region (e.g., Egypt) and providing news from the same categories (e.g., business) exhibit high correlation.

Quality Initialization. We examine how the output of SLiMFAST, can be used to answer the problem of source quality initialization [21], i.e., the task of estimating the accuracy of newly available sources, from which no observations are available. We use the learned weights of domain-specific features to predict the accuracy of new sources. We conduct the following experiment: for Stock, Demonstrations and Crowd, we restrict the number of sources given as input to SLiMFAST, varying the percentage of used sources in $\{25\%, 40\%, 50\%, 75\%\}$. After learning the model parameters the feature weights are used to predict the accuracy of unseen sources. The results are shown in Figure 13. We see that the estimation error decreases as more sources are revealed to SLiMFAST. For Stocks and Demonstrations, the error is larger compared to the case when we have access to the data of a source. For Crowd we can reliably predict the accuracy of unseen data sources even when only 25% of all sources are available.

Data Fusion and Unstructured Data. A shortcoming of all existing data fusion approaches is their assumption that entity resolution across objects mentioned in source observations has been

performed in advance. However, this is not the case for most real applications that require extracting information from raw textual data. Leveraging the fact that SLiMFAST is implemented on top of DeepDive, we integrate SLiMFAST with a pipeline that extracts information from unstructured data and examine its effect on the quality of the pipeline’s output. This unified framework reasons about the uncertainty of extractions and the accuracy of data sources in a joint manner. We found that data fusion can lead to more accurate extractions. Our results are presented in detail in Appendix D.1.

7. RELATED WORK

The prior work related to this paper can be placed in a few categories; we describe each of them in turn:

Data fusion. There has been a significant amount of work on data fusion models, including approaches that follow probabilistic semantics [6, 7, 27, 40], optimization-based techniques [18, 19], and iterative models [12, 26, 37]. A common theme across all methods is resolving source conflicts by first estimating the reliability of each available source—sometimes measured as the source’s accuracy. We show that several of these models can be thought of as a logistic regression model. This approach lets us leverage external domain specific signals for obtaining better source accuracy estimates; previous works do not use such external signals. Combining both types of signals has been recently identified as a potential direction for designing improved data fusion methods [7].

Quality guarantees for data fusion. Several of the existing data fusion methods come with guarantees on their convergence [6] or come with confidence intervals for the estimated source accuracy [18]. Nevertheless, no existing method comes with guarantees on how close the estimated source accuracies are to the *true accuracies of data sources*. From the interviews we conducted, we found that non-expert users — especially from fields such as biology or medicine — require that automated techniques be coupled with rigorous guarantees before using them in downstream applications. Our approach lets us leverage existing results from learning theory to obtain guarantees on the error rate of our source accuracy estimates, as well as our object truth estimates. The only work prior to ours that comes with theoretical guarantees on the error rate of accuracy estimates is from the crowdsourcing community [5, 14, 15, 23] where data sources correspond to human workers. In fact, recent work in crowdsourcing [13, 39] showed that EM-based Bayesian data fusion models can retrieve the true accuracies of data sources with a convergence error of $O\left(\sqrt{s \log(s)/n}\right)$ where s denotes the number of sources and n the number of source data entries. Nevertheless, these results come with several strong assumptions on the range of values source accuracy can take and the number of sources or objects in the fusion instance. Also, none of the proposed approaches considers exogenous features characterizing human workers. Our techniques might be of independent interest to the crowdsourcing community.

Explanations for data fusion. Understanding the output of data fusion is crucial for non-expert users [21]. Recent work [9] has considered the problem of providing explanations on the output of data fusion algorithms. The generated explanations correspond to compact summaries of the decisions made by the fusion algorithm during its execution. The summaries are also coupled with examples from the input source data to promote interpretability. In our work we follow an orthogonal direction. Instead of relying on source data and presenting the user with a trace of the fusion algorithm, we leverage the presence of domain specific features, and

use techniques like L1-regularization [35] to present users with the most informative features that affect source accuracies.

Efficiency of data fusion. Most existing data fusion methods adopt iterative procedures like EM to estimate the quality of sources and compute the true values of objects [21]. This can be very time consuming, especially when data fusion is applied on large scale data [20]. To address this challenge, recent literature has proposed the use of Map-Reduce based techniques [7] and has introduced streaming data fusion methods [41]. When sufficient ground truth is available, we can avoid time consuming iterative algorithms entirely by using Empirical Risk Minimization. Our optimizer allows us to choose appropriately between these two approaches, based on the amount of ground truth available.

8. CONCLUSION

We expressed data fusion as a learning and inference problem over discriminative probabilistic graphical models. This enabled us to obtain data fusion models with rigorous guarantees and answer a series of open problems in data fusion. We introduced SLiMFAST, the first model that combines cross-source conflicts with domain-specific features for data fusion. Our theoretical and experimental analysis showed that domain-specific features not only lead to better source accuracy estimates but also allow us to identify the true value of objects more accurately.

We also studied the tradeoff space between the runtime and model quality of expectation maximization (EM)—a standard technique for learning the parameters of data fusion models—and empirical risk minimization (ERM) that uses ground truth data to learn the model parameters. We proposed a simple information theoretic model for estimating the performance of each algorithm and built an optimizer that automatically selects the best algorithm for learning the parameters of a given data fusion model. Our experiments confirmed the effectiveness of our optimizer for a variety of data fusion setups. Finally, we showed SLiMFAST can make data fusion more practical and more approachable to non-expert users.

9. REFERENCES

- [1] <https://alchemy.cs.washington.edu/>.
- [2] <http://deepdive.stanford.edu/>.
- [3] F. Bach, R. Jenatton, J. Mairal, and G. Obozinski. Optimization with sparsity-inducing penalties. *Found. Trends Mach. Learn.*, 4:1–106, 2012.
- [4] J. Bleiholder and F. Naumann. Data fusion. *ACM Comput. Surv.*, 41:1:1–1:41, 2009.
- [5] N. Dalvi, A. Dasgupta, R. Kumar, and V. Rastogi. Aggregating crowdsourced binary ratings. In *WWW*, 2013.
- [6] X. L. Dong, L. Berti-Equille, and D. Srivastava. Integrating conflicting data: The role of source dependence. *VLDB*, 2:550–561, 2009.
- [7] X. L. Dong, E. Gabrilovich, K. Murphy, V. Dang, W. Horn, C. Lugaresi, S. Sun, and W. Zhang. Knowledge-based trust: Estimating the trustworthiness of web sources. *VLDB*, 8:938–949, 2015.
- [8] X. L. Dong, B. Saha, and D. Srivastava. Less is more: selecting sources wisely for integration. In *VLDB*, pages 37–48, 2013.
- [9] X. L. Dong and D. Srivastava. Compact explanation of data fusion decisions. In *WWW*, pages 379–390, 2013.
- [10] X. L. Dong and D. Srivastava. *Big Data Integration*. Synthesis Lectures on Data Management. 2015.
- [11] J. Friedman, T. Hastie, and R. Tibshirani. Regularization paths for generalized linear models via coordinate descent. *Journal of Statistical Software*, 33:1–22, 2010.
- [12] A. Galland, S. Abiteboul, A. Marian, and P. Senellart. Corroborating information from disagreeing views. In *WSDM*, pages 131–140, 2010.
- [13] C. Gao and D. Zhou. Minimax optimal convergence rates for estimating ground truth from crowdsourced labels. Technical Report MSR-TR-2013-110, October.
- [14] M. Joglekar, H. Garcia-Molina, and A. Parameswaran. Evaluating the crowd with confidence. In *KDD*, pages 686–694, 2013.
- [15] D. Karger, S. Oh, and D. Shah. Iterative learning for reliable crowdsourcing systems. In *NIPS*, pages 1953–1961. 2011.
- [16] A. Kimmig, S. H. Bach, M. Broecheler, B. Huang, and L. Getoor. A short introduction to Probabilistic Soft Logic. In *NIPS Workshop on Probabilistic Programming*, 2012.
- [17] K. Leetaru and P. Schrodt. GDEL: Global Database of Events, Language, and Tone. In *ISA Annual Convention*, 2013.
- [18] Q. Li, Y. Li, J. Gao, L. Su, B. Zhao, M. Demirbas, W. Fan, and J. Han. A confidence-aware approach for truth discovery on long-tail data. *Proc. VLDB Endow.*, 8(4):425–436, Dec. 2014.
- [19] Q. Li, Y. Li, J. Gao, B. Zhao, W. Fan, and J. Han. Resolving conflicts in heterogeneous data by truth discovery and source reliability estimation. *SIGMOD '14*, pages 1187–1198, 2014.
- [20] X. Li, X. L. Dong, K. Lyons, W. Meng, and D. Srivastava. Truth finding on the deep web: is the problem solved? In *VLDB*, pages 97–108, 2013.
- [21] Y. Li, J. Gao, C. Meng, Q. Li, L. Su, B. Zhao, W. Fan, and J. Han. A survey on truth discovery. *SIGKDD Explor. Newsl.*, 17(2), 2016.
- [22] P. Liang. <https://web.stanford.edu/class/cs229/notes.pdf>.
- [23] A. P. M. Joglekar, H. Garcia-Molina. Comprehensive and reliable crowd assessment algorithms. In *ICDE*, 2015.
- [24] T. M. Mitchell. *Machine Learning*. 1997.
- [25] A. Y. Ng and M. I. Jordan. On discriminative vs. generative classifiers: A comparison of logistic regression and naive bayes. In *NIPS*, pages 841–848. MIT Press, 2002.
- [26] J. Pasternack and D. Roth. Knowing what to believe (when you already know something). In *COLING*, pages 877–885, 2010.
- [27] J. Pasternack and D. Roth. Latent credibility analysis. In *WWW*, pages 1009–1020, 2013.
- [28] A. B. Patel, T. Nguyen, and R. G. Baraniuk. A probabilistic theory of deep learning. *arXiv preprint arXiv:1504.00641*, 2015.
- [29] N. Ramakrishnan, C. Lu, M. Marathe, A. Marathe, A. Vullikanti, S. Eubank, S. Leman, M. Roan, J. Brownstein, K. Summers, et al. Model-based forecasting of significant societal events. *Intelligent Systems, IEEE*, 30:86–90, 2015.
- [30] T. Rekatsinas, S. Ghosh, S. Mekar, E. Nsoesie, J. Brownstein, L. Getoor, and N. Ramakrishnan. Sourceeer: Forecasting rare disease outbreaks using multiple data sources. In *SDM*, 2015.
- [31] C. D. Sa, C. Ré, and K. Olukotun. Global convergence of stochastic gradient descent for some non-convex matrix problems. In *ICML 2015*, pages 2332–2341, 2015.
- [32] R. Samdani, M.-W. Chang, and D. Roth. Unified expectation maximization. *NAACL HLT '12*, 2012.
- [33] J. Shin, S. Wu, F. Wang, C. De Sa, C. Zhang, and C. Ré. Incremental knowledge base construction using DeepDive. *Proc. VLDB Endow.*, 8(11):1310–1321, July 2015.
- [34] C. Sutton and A. McCallum. An introduction to conditional random fields. *Found. Trends Mach. Learn.*, 4(4):267–373, Apr. 2012.
- [35] R. Tibshirani. Regression shrinkage and selection via the lasso. pages 267–288, 1996.
- [36] C. J. Wu. On the convergence properties of the EM algorithm. *The Annals of statistics*, pages 95–103, 1983.
- [37] X. Yin, J. Han, and P. Yu. Truth discovery with multiple conflicting information providers on the web. In *KDD*, pages 1048–1052, 2007.
- [38] C. Zhang and C. Ré. Dimm-witted: A study of main-memory statistical analytics. *PVLDB*, pages 1283–1294, 2014.
- [39] Y. Zhang, X. Chen, D. Zhou, and M. I. Jordan. Spectral methods meet EM: A provably optimal algorithm for crowdsourcing. In *NIPS*, pages 1260–1268. 2014.
- [40] B. Zhao, B. Rubinstein, J. Gemmell, and J. Han. A bayesian approach to discovering truth from conflicting sources for data integration. *VLDB*, 5:550–561, 2012.
- [41] Z. Zhao, J. Cheng, and W. Ng. Truth discovery in data streams: A single-pass probabilistic approach. In *CIKM*, pages 1589–1598, 2014.

APPENDIX

A. RADEMACHER COMPLEXITY

We let \mathcal{L} denote the set of L_w for all $|K|$ -dimensional vectors w .

We introduce the notion of Rademacher complexity [22], which measures the richness of a class of functions and is used for excess risk bounds and generalization bounds. The Rademacher complexity of a set of functions \mathcal{H} and a training set size n is given by:

$$\mathcal{R}_n(\mathcal{H}) = (2/n)E_{\sigma_1, \dots, \sigma_n}[\sup_{h \in \mathcal{H}} (|\sum_{i=1}^n \sigma_i h(z_i)|)]$$

where σ_i for $1 \leq i \leq n$ are independent random variables that take value 1 or -1 with probability $1/2$ each, and z_i s are n i.i.d training samples drawn from a distribution \mathcal{D} . For our setting, \mathcal{H} is simply \mathcal{L} , and the z_i 's are source-object pairs. $h(z_i)$ is simply $L_w(s, o)$. Since our loss is a function of a linear function of parameters w and those of the source object pairs, we can use a well known bound on the Rademacher complexity of our class of loss functions. Specifically:

$$\mathcal{R}_n(\mathcal{L}) = O(\sqrt{|K|/n} \log(n)) \quad (4)$$

Now we state an excess risk bound that uses Rademacher complexity. For any function class \mathcal{H} , for a set S of n i.i.d training samples z_1, z_2, \dots, z_n from distribution \mathcal{D} , the empirical risk minimizer is defined as:

$$h_{erm} = \operatorname{argmin}_{h \in \mathcal{H}} \sum_{i=1}^n h(z_i)$$

Moreover, let the optimal function be

$$h_{\infty} = \operatorname{argmin}_{h \in \mathcal{H}} E_{z \sim \mathcal{D}}[h(z)]$$

Then with high probability (over the draws of z_i s), we have [22]:

$$E_{z \sim \mathcal{D}}[h_{erm}(z)] \leq E_{z \sim \mathcal{D}}[h_{\infty}(z)] + O(\mathcal{R}_n(\mathcal{H})) \quad (5)$$

Rademacher complexity also lets us quantify the rate of *uniform convergence*. Specifically, for any $h \in \mathcal{H}$, let

$$h(S) = (1/|S|) \sum_{z \in S} h(z)$$

and

$$h_E = E_{z \sim \mathcal{D}}[h(z)]$$

When $S \sim \mathcal{D}^m$, we would like to upper bound $\max_{h \in \mathcal{H}} |h(S) - h_E|$ as a function of m . For any δ in $(0, 1)$, we have with probability $\geq 1 - \delta$,

$$\max_{h \in \mathcal{H}} |h(S) - h_E| \leq 2\mathcal{R}_n(\mathcal{H}) + \sqrt{\log(1/\delta)/2n} \quad (6)$$

B. PROOFS

We provide the proofs for the theorems in Section 3.

B.1 Proof of Theorem 1

In our setting, $E_{z \sim \mathcal{D}}[h_{erm}(z)]$ from Equation 5 is simply L_w , while $E_{z \sim \mathcal{D}}[h_{\infty}(z)]$ is L_{w^*} , and \mathcal{H} is the family of losses for all weight vectors. Then applying Equation 4 to the $\mathcal{R}_n(\mathcal{H})$ term gives us Theorem 1.

B.2 Proof of Theorem 2

This theorem follows from the uniform convergence result in Equation 6. For any constant δ , the $\sqrt{\log(1/\delta)/2n}$ term is subsumed by the $\mathcal{R}_n(\mathcal{H})$ term, because for our case,

$$\mathcal{R}_n(\mathcal{H}) = O(\sqrt{|K|/n} \log(n))$$

due to Equation 4. Thus we simply have, for any $h' \in \mathcal{H}$,

$$|h'(S) - h'_E| \leq \max_{h \in \mathcal{H}} |h(S) - h_E| \leq O(\sqrt{|K|/n} \log(n))$$

Replacing $h(S)$ by $L_G(w)$ and h_E by $L(w)$ gives us our theorem.

B.3 Proof of Theorem 3

We start by considering two cases, based on the probability p of a source observing an object. If $p = \omega(\log(n)/\delta)$, then with high probability, the majority value of observations on each object equals the true value of the object. In this case, we can just compute the majority and treat it as ground truth, and apply Theorem 1. The number of labeled source-object pairs in this case is $O(|S||O|p)$, substituting $n = |S||O|p$ that value gives us our required result. The second case is where $p = O(\log(n)/\delta)$. In this case we drop objects that have < 2 observations, and for other objects, randomly drop all but two observations. This reduces the problem to a slightly different problem, which is easier to solve. We now solve the reduced problem in the rest of the section.

The reduced problem is as follows: We have $n = |O|$ objects. For each object, we choose a pair of sources uniformly at random, and both the chosen sources make an observation on the object. In this case, we show that we can estimate source accuracies such that

$$\frac{1}{|S|} \sum_{s \in S} KL(A_s \| A_s^*) \leq O(\log(|O|)/(|S|\delta) + \sqrt{k/|O||S|} \log(|O||S|))$$

. This, along with $p = O(\sqrt{n}/\delta)$, will prove our theorem.

For each object o , we randomly designate one of its two observing sources as 'primary', denoted $S(o)$. For any source s , let O_s denote the set of objects such that $S(o) = s$. For any object o , let $\text{Agree}(o)$ equal 1 if the two sources observing o agreed on it, and 0 otherwise.

Our accuracy estimation algorithm has three steps:

1. Estimate $A_E = \sum_{s \in S} (2A_s^* - 1)$. Let A'_E denote our estimate.
2. For each source s , compute $a_s = (\sum_{o \in O_s} (2|S|\text{Agree}(o) - (|S| - A'_E))) / 2A'_E$.
3. Choose w to minimize $\sum_{s \in S} a_s \log(\logistic(w \cdot F_s)) + (|O_s| - a_s) \log(1 - \logistic(w \cdot F_s))$.

Then we prove that the chosen w from the third step must be such that accuracy estimates $A_s = \logistic(w \cdot F_s)$ satisfy our guarantee.

Step 1: We first show that step 1 can be carried out, such that our estimate A'_E has a relative error of $O(1/|S|\delta + 1/\sqrt{n})$, with high probability. Relative error of ϵ here means that A'_E is in interval $((1 - \epsilon)A_E, (1 + \epsilon)A_E)$.

To begin with, note that $2A_s^* - 1 \in [\delta, 1 - \delta]$ for all s . For any $o \in O$, the expected value $E[\text{Agree}(o)]$ is

$$(1/|S|(|S| - 1)) \sum_{s_1, s_2 \in S, s_1 \neq s_2} A_{s_1}^* A_{s_2}^* + (1 - A_{s_1}^*)(1 - A_{s_2}^*)$$

since the pair of sources is chosen randomly, and sources s_1 and s_2 agree on an object if they are both correct or both wrong. Moreover,

$A_{s_1}^* A_{s_2}^* + (1 - A_{s_1}^*)(1 - A_{s_2}^*)$ equals $1/2 + (2A_{s_1}^* - 1)(2A_{s_2}^* - 1)/2$. Thus expected value of $2|S|(|S| - 1)\text{Agree}(o)$ is

$$\begin{aligned} & 2 \sum_{s_1, s_2 \in S, s_1 \neq s_2} A_{s_1}^* A_{s_2}^* + (1 - A_{s_1}^*)(1 - A_{s_2}^*) \\ &= \sum_{s_1, s_2 \in S, s_1 \neq s_2} 1 + (2A_{s_1}^* - 1)(2A_{s_2}^* - 1) \\ &= \sum_{s_1, s_2 \in S} 1 + (2A_{s_1}^* - 1)(2A_{s_2}^* - 1) - \sum_{s \in S} 1 + (2A_s^* - 1)^2 \\ &= |S|(|S| - 1) + \sum_{s_1, s_2 \in S} (2A_{s_1}^* - 1)(2A_{s_2}^* - 1) - \sum_{s \in S} (2A_s^* - 1)^2 \\ &= |S|(|S| - 1) + \left(\sum_{s \in S} (2A_s^* - 1) \right)^2 - \sum_{s \in S} (2A_s^* - 1)^2 \\ &= |S|(|S| - 1) + A_E^2 - \sum_{s \in S} (2A_s^* - 1)^2 \end{aligned}$$

Thus expected value of $|S|(|S| - 1)(2\text{Agree}(o) - 1)$ equals $A_E^2 - \sum_{s \in S} (2A_s^* - 1)^2$. Moreover, $A_E \geq |S|\delta$ and $2A_s^* - 1 \leq 1$ for all s , so

$$\begin{aligned} A_E^2 &= \sum_{s \in S} (2A_s^* - 1)A_E \\ &\geq \sum_{s \in S} (2A_s^* - 1)|S|\delta \\ &\geq \sum_{s \in S} (2A_s^* - 1)|S|\delta(2A_s^* - 1) \\ &= \sum_{s \in S} (2A_s^* - 1)^2 |S|\delta \end{aligned}$$

This gives us

$$A_E^2 \geq A_E^2 - \sum_{s \in S} (2A_s^* - 1)^2 \geq A_E^2(1 - 1/(|S|\delta))$$

So we can estimate A_E by computing

$$|S|(|S| - 1)/|O| \left(\sum_{o \in O} 2\text{Agree}(o) - 1 \right)$$

and taking it's square root. Since the sum over $o \in O$ involves i.i.d variables, we can use the Chernoff bound, showing that the sum, and hence estimate of A_E , has a relative error of $O(1/(|S|\delta) + 1/\sqrt{n})$. Let A'_E denote our noisy estimate of A_E obtained above. This completes step 1.

Step 2,3: Step 2 is simple, and is used to compute the loss function in Step 3. We now show that the w 's computed in step 3 give accurate estimates. For that, we need to define two loss functions, L_1 and L_2 . L_1 will be the loss function we actually care about (log-loss of source accuracies). However, we cannot directly estimate L_1 without ground truth. So we will define another loss function L_2 , which will be shown to be close to L_1 , and which can be estimated from samples of source conflicts.

First, we define $L_1(w) = (1/|S|) \sum_{s \in S} A_s^* \log(\text{logistic}(w \cdot F_s)) + (1 - A_s^*) \log(1 - \text{logistic}(w \cdot F_s))$. The weights w^* that minimize this loss function are precisely the weights that give us $A_s^* = \text{logistic}(w^* \cdot F_s)$ for all s . Unfortunately, we cannot empirically estimate this loss directly.

In step 3, we minimize the 'empirical' loss function $L_{emp}(w)$ given by $\sum_{s \in S} a_s \log(\text{logistic}(w \cdot F_s)) + (|O_s| - a_s) \log(1 - \text{logistic}(w \cdot F_s))$.

$L_{emp}(w)$ can also be written as $\sum_{o \in O} a_o \log(\text{logistic}(w \cdot F_{S(o)})) + (1 - a_o) \log(1 - \text{logistic}(w \cdot F_{S(o)}))$ where

$$a_o = (2|S|\text{Agree}(o) - (|S| - A'_E))/2A'_E$$

We now define a loss L_2 such that the $L_{emp}(w)$ is a 'sampled' version of L_2 . Specifically, define $L_2(w)$ to be:

$$E[a_o \log(\text{logistic}(w \cdot F_{S(o)})) + (1 - a_o) \log(1 - \text{logistic}(w \cdot F_{S(o)}))]$$

where the expectation is taken over objects (random choices over the sources that observe the object, and over the observations of those sources). For any object $o \in O_s$, we define B_s^* such that

$$B_s^* = (1/(2|S| - 2))(|S| - 1 + (2A_s^* - 1)(A_E - 2A_s^* + 1))$$

Thus, we have $E[\text{Agree}(o)] = B_s^*$. So

$$E_{o \in O_s}[a_o] = (2|S|B_s^* - (|S| - A'_E))/2A'_E$$

Moreover, we now have

$$\begin{aligned} L_2(w) &= (1/|S|) \left(\sum_{s \in S} (2|S|B_s^* - (|S| - A'_E)) \log(\text{logistic}(w \cdot F_s)) / 2A'_E \right. \\ &\quad \left. + (1 - (2|S|B_s^* - (|S| - A'_E))) / 2A'_E \log(1 - \text{logistic}(w \cdot F_s)) \right) \end{aligned}$$

Our proof now proceeds in two steps. (a) We show that L_1 and L_2 are very close, upto scaling (b) We show that the weight vector w chosen to minimize $L_{emp}(w)$, also achieves a very low value for L_2 , using standard Rademacher complexity bounds.

We show (b) first, since it is straightforward. We choose w_e to minimize L_{emp} , i.e. $w_e = \text{argmin}_w \sum_{o \in O} a_o \log(\text{logistic}(w \cdot F_{S(o)})) + (1 - a_o) \log(1 - \text{logistic}(w \cdot F_{S(o)}))$. Now L_2 is simply the expected value of this quantity. Let \mathcal{L} denote the family of $L_2(w)$ over all w . Then, since each member of the family consists of a function of a linear function of w , the Rademacher complexity $\mathcal{R}_n(\mathcal{L}) = O(\sqrt{k/n} \log(n))$. Thus,

$$L_2(w_e) \leq L_2(w') + O(\sqrt{k/n} \log(n))$$

where w' is the weight vector that minimizes $L_2(w)$.

Now we show (a). To begin with, we will show that B_s^* is very close to $(1/2|S|)(|S| + (2A_s^* - 1)A_E)$. We have $B_s^* = (1/(2|S| - 2))(|S| - 1 + (2A_s^* - 1)(A_E - 2A_s^* + 1))$, so

$$\begin{aligned} & |B_s^* - (1/2|S|)(|S| + (2A_s^* - 1)A_E)| \\ &= 1/(2|S|(|S| - 1))(|S|(|S| - 1) + |S|(2A_s^* - 1)(A_E - 2A_s^* + 1)) \\ &\quad - |S|(|S| - 1) + (|S| - 1)(2A_s^* - 1)A_E) \\ &= 1/(2|S|(|S| - 1))(2A_s^* - 1)(|S|(A_E - 2A_s^* + 1) - (|S| - 1)A_E) \\ &= 1/(2|S|(|S| - 1))(2A_s^* - 1)(|A_E - |S|(2A_s^* - 1)|) \\ &\leq 1/(2|S|(|S| - 1))(2A_s^* - 1)|S| \\ &\leq 1/(2|S| - 2) \end{aligned}$$

Since $B_s^* \geq 1/2$, it means that $B = (1/2|S|)(|S| + (2A_s^* - 1)A_E)$ estimates all B_s^* with a relative error of $\leq 1/(|S| - 1)$. Moreover, we saw earlier that A'_E estimates A_E with relative error of $O(1/(|S|\delta) + 1/\sqrt{n})$. Also note that if we replace B_s^* with B

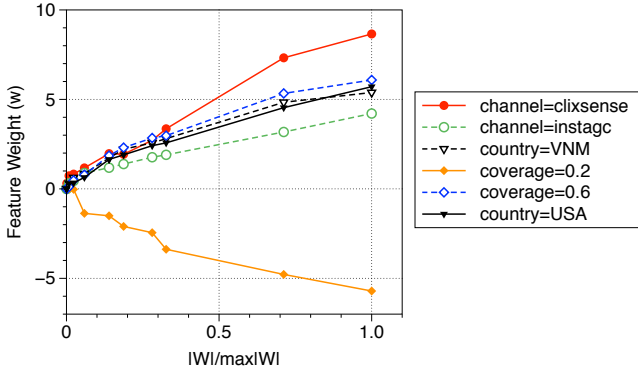


Figure 14: Lasso path for features used in Crowd. Higher x -axis values correspond to lower regularization penalties.

and A'_E with A_E in L_2 , then it would become equal to L_1 . This is because

$$\begin{aligned}
& (2|S|B - (|S| - A_E))/2A_E \\
&= 2|S|((1/2|S|)(|S| + (2A_s^* - 1)A_E)) - (|S| - A_E)/2A_E \\
&= (|S| + (2A_s^* - 1)A_E) - (|S| - A_E)/2A_E \\
&= (|S| + 2A_s^*A_E - A_E - |S| + A_E)/2A_E \\
&= (2A_s^*A_E)/2A_E \\
&= A_s^*
\end{aligned}$$

Similarly, the other term (corresponding to $1 - a_o$) becomes $1 - A_s^*$. With this insight, we can show that L_1 and L_2 are close. The numerator, as seen above, was equal to $2A_s^*A_E \geq 2(1/2)|S|\delta$ (since $A_E \geq |S|\delta$). The multiplicative error in the $2|S|B$ term is $1/(|S| - 1)$, thus absolute error is $O(1)$ since $B < 1$. This will cause a relative error of $O(1/(|S|\delta))$ in numerator $2A_s^*A_E$. Similarly, relative error in A'_E is $1/(|S|\delta) + 1/\sqrt{n}$, which causes a relative error of $1/(|S|\delta) + 1/\sqrt{n}$ in $2A_s^*A_E$. Thus the total relative error in $2A_s^*A_E$ is at most $O(1/(|S|\delta) + 1/\sqrt{n})$. We can show a similar result for the second terms of L_1 and L_2 . Thus L_2 approximates L_1 with a relative error of $O(1/(|S|\delta) + 1/\sqrt{n})$. Moreover, any w we consider for learning with n samples will satisfy $\log(\text{logistic}(w \cdot F_s)) = O(\log(n))$. Thus for any such w , $|L_1(w) - L_2(w)| = O(\log(n)/(|S|\delta) + \log(n)/\sqrt{n})$.

Now, let w^* be the weights that give us true accuracies i.e. $A_s^* = \text{logistic}(w^* \cdot F_s)$. And, w_e is the weight chosen by our algorithm. Then

$$\begin{aligned}
L_1(w_e) &\leq L_2(w_e) + O(\log(n)/(|S|\delta) + \log(n)/\sqrt{n}) \\
&\leq L_2(w') + O(\sqrt{k/n} \log(n)) + O(\log(n)/(|S|\delta) + \log(n)/\sqrt{n}) \\
&\leq L_2(w^*) + O(\sqrt{k/n} \log(n)) + O(\log(n)/(|S|\delta) + \log(n)/\sqrt{n}) \\
&\leq L_1(w^*) + O(\sqrt{k/n} \log(n)) + O(\log(n)/(|S|\delta) + \log(n)/\sqrt{n})
\end{aligned}$$

The first and last step uses the closeness of L_1 and L_2 . The second step uses the Rademacher complexity excess risk bound given earlier. The third step is because w' is defined as the w that minimizes L_2 . This shows that our chosen w_e will L_1 loss value which is not much worse than that of the best weights w^* .

Moreover, $L_1(w) - L_1(w^*)$ is simply the average KL divergence with true accuracies. i.e.

$$L_1(w_e) - L_1(w^*) = (1/|S|) \sum_{s \in S} KL(A_s || A_s^*)$$

where $A_s = \text{logistic}(w_e \cdot F_s)$. This gives us

$$(1/|S|) \sum_{s \in S} KL(A_s || A_s^*) = O(\log(n)/(|S|\delta) + \sqrt{k/n} \log(n))$$

This proves our claim, and using $p = O(\log(n)/\delta)$ finishes our proof for the theorem.

C. FEATURE SELECTION

Our previous bound on Kullback-Leibler divergence shows that it is proportional to $\sqrt{|K|}$. This suggests that adding extra, potentially uninformative features to our model can significantly worsen our source accuracy estimates by increasing $|K|$. A user has no way of knowing in advance, which features will be informative and which ones will be uninformative. Fortunately, it is possible for a user to add lots of features to the model, without incurring a large increase in accuracy estimation error, as long as we regularize our model appropriately.

L_1 -regularization is a well known way to induce sparsity in the solution [3], i.e., to have only a small number of non-zero values in the weight vector w . If the user provides a large number of features, of which only a few are predictive of source accuracy, then using l_1 -regularization allows us to obtain a weight vector w that only assigns non-zero weights to the predictive features. Moreover, in this case, we can show that the error in the accuracy estimate is proportional to the square root of the number of predictive features, rather than the square root of the total number of features. Formally, if k of the $|K|$ features get non-zero weight, then we have:

$$L_w \leq L_{w^*} + O(\sqrt{k \log(|K|)/n} \log(n)) \quad (7)$$

D. LASSO PATH FOR CROWD

Figure 14 shows the lasso path plot for features used in Crowd. We show the paths for the first two features from channel, city and coverage that activated. The first feature that activates is channel “clixsense”. Also it is interesting to observe that “coverage=0.6” (relatively high coverage) has a high positive weight while “coverage=0.2” (low coverage) has a high negative weight.

D.1 Information Extraction Pipelines

We focus on extracting relations between people and organizations from 2.4 million news articles from Eventregistry.org. Articles span the period from June, 2014 to March, 2015. The entire extraction and fusion pipeline was implemented using DDlog, DeepDive’s declarative language. We describe the key steps in the pipeline and then report our findings.

To extract raw person-organization relations we tokenized each news article into sentences and applied standard NLP tools on each sentence to identify person and organization mentions connected via a phrase that reveals a relation (e.g., “head of”, “manager of”, “counsel of” etc.). Both person mentions and organization mentions can be noisy due to extraction errors or obfuscated mentions in the news article themselves. Moreover, news articles may report erroneous fact. Each extraction corresponds to a tuple $r = \{per, org, rel\}$. We associate each extraction with the news domain it was obtained from (i.e., the data source) and several textual features, e.g., the words between the person and organization mentions, readability ease metrics etc. To determine if two extractions correspond to the same real-world latent object we encode entity resolution in our pipeline. The entity resolution rules are shown in Figure 15. The same figure shows the calibration plots with and without data fusion. Data fusion leads to results that are better calibrated, i.e., exhibit higher accuracy with respect to available ground truth data.

Entity Resolution and Data Fusion Rules for Person-Organization Relation Extraction

$w_1 :$	$r.per \simeq r'.per \wedge r.org \simeq r'.org \wedge r.rel \simeq r'.rel \implies r = r'$	
$w_2 :$	$r.per \simeq r'.per \wedge r.org \simeq r'.org \wedge \neg(r.rel \simeq r'.rel) \implies r \neq r'$	
$w_3 :$	$r.per \simeq r'.per \wedge \neg(r.org \simeq r'.org) \wedge r.rel \simeq r'.rel \wedge \text{ExclRel}(r.rel) \implies r \neq r'$	
$w(r.src) :$	$\text{IsTrue}(r) \wedge r = r' \implies \text{IsTrue}(r)$	\simeq : Fuzzy String Match
$w(r.src) :$	$\text{IsTrue}(r) \wedge r \neq r' \implies \neg\text{IsTrue}(r)$	$=$: Agreement
		\neq : Disagreement

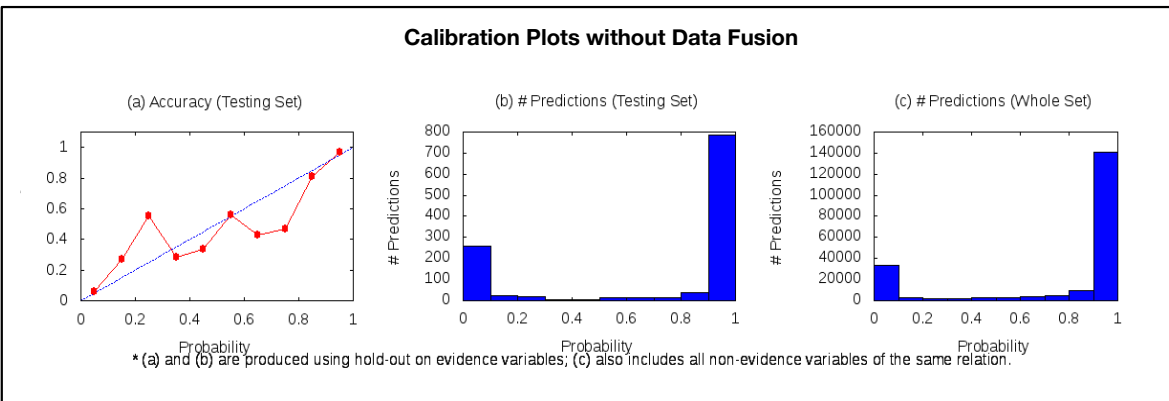
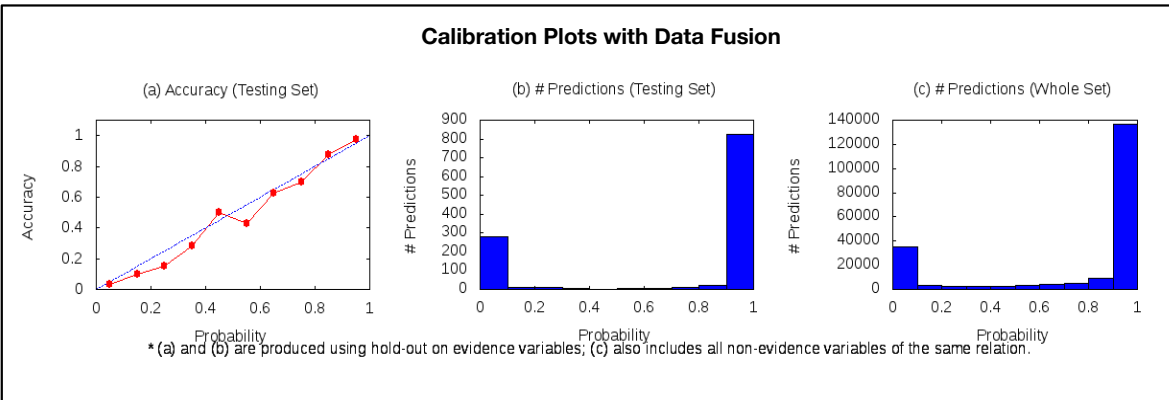


Figure 15: Integrating data fusion with information extraction.